

CARBON DEFICIENCY IN EXTERNALLY-POLLUTED WHITE DWARFS: EVIDENCE FOR ACCRETION OF ASTEROIDS

M. Jura

Department of Physics and Astronomy and Center for Astrobiology
University of California, Los Angeles CA 90095-1562; jura@astro.ucla.edu

ABSTRACT

Existing determinations show that $n(\text{C})/n(\text{Fe})$ is more than a factor of 10 below solar in the atmospheres of three white dwarfs that appear to be externally-polluted. These results are not easily explained if the stars have accreted interstellar matter, and we re-interpret these measurements as evidence that these stars have accreted asteroids with a chondritic composition.

Subject headings: planetary systems – white dwarfs

1. INTRODUCTION

In white dwarfs with effective temperatures lower than about 20,000 K, it is predicted that heavy elements settle below the photosphere in the star's strong gravitational field so the atmosphere is either largely hydrogen or largely helium (Paquette et al. 1986, Chayer et al. 1995). This expectation is supported by the determination that $\sim 75\%$ of these stars display upper limits to their calcium abundance that are as much as a factor of 10^6 below the solar value (Zuckerman et al. 2003). Currently, the only viable hypothesis to explain the observational result that $\sim 25\%$ of cool white dwarfs have detected metals is that these stars are externally-polluted. Interstellar accretion (Paquette et al. 1986, Dupuis et al. 1993a,b, Koester & Wilken 2006) is often thought to account for the metals within white dwarf atmospheres, but accretion from a tidally-disrupted minor body such as an analog to an asteroid or Kuiper Belt Object naturally explains the infrared excesses and metal pollutions of the hydrogen-rich white dwarfs G29-38, GD 362 and GD 56 (Jura 2003, Becklin et al. 2005, Kilic et al. 2005, 2006, Reach et al. 2005). Here we re-interpret existing abundance determinations of three helium-rich white dwarfs that previously were thought to have accreted interstellar matter to argue, instead, that their measured low values of $n(\text{C})/n(\text{Fe})$ support the hypothesis that these stars have accreted circumstellar matter with a chondritic composition.

Since the diffusion times out of a white dwarf’s atmosphere for different elements heavier than helium vary by less than a factor of 2.5 (Paquette et al. 1986, Dupuis et al. 1993a), a test of any accretion scenario is to compare the metals in the star’s photosphere with the composition of the polluter. Within meteorites of all kinds as well as the Earth’s crust, carbon is depleted relative to refractory species such as iron, magnesium and silicon by at least a factor of 10 and often more. Accretion of circumstellar matter with a composition similar to rocky material in the inner solar system can lead to distinctively low values of $n(\text{C})/n(\text{Fe})$ that cannot be naturally explained by accretion of interstellar matter. On the basis of this argument, a carbon deficiency in the photosphere of the main sequence star J37 in the open cluster NGC 6633 has been attributed to the accretion of material with a chondritic composition (Ashwell et al. 2005, Laws & Gonzalez 2003).

Carbon has been detected in some helium-rich white dwarfs. For the stars with $T_{eff} < 13000$ K, the convective zones are sufficiently deep that carbon may be dredged up from the interior (Koester et al. 1982, Pelletier et al. 1986, Dupuis et al. 1993b, MacDonald et al. 1998). In three white dwarfs with T_{eff} near 25000 K, Petitclerc et al. (2005) have reported an unexplained presence of enhanced carbon with, for example, $n(\text{C})/n(\text{Si}) > 100$. Here we focus on stars with carbon deficiencies in the sense that $n(\text{C}) \ll n(\text{Fe})$.

The unique chemistry of carbon makes it a useful element for distinguishing between circumstellar and interstellar models of atmospheric pollution. In the early solar system, carbon was probably largely concentrated in volatile molecules such as CH_4 and CO (see, for example, Lodders 2003, 2004) and not incorporated into rocky bodies that formed in the inner solar system such as the Earth and asteroids (see also Simonelli et al. 1997, Gail 2002). In environments where carbon is more abundant than oxygen, carbon can condense into refractory solids such as graphite, and this may have occurred during the formation of some of the outer regions of the solar system where water was depleted (see Krot et al. 2000) and also, perhaps, around β Pic (Roberge et al. 2006). In any case, meteorites, which are the best available measure of the composition of asteroids, are deficient in carbon (Wasson & Kallemeyn 1988). In contrast, as discussed below, carbon is abundant in both the gaseous and solid phase in the interstellar medium.

In §2 we discuss scenarios for interstellar accretion and describe why the alternative of accretion from circumstellar matter is preferable for many stars. In §3 we describe the scenario for white dwarf pollutions by minor bodies such as asteroids. In §4 we discuss our results and in §5 we report our conclusions.

Below, we suggest that at least 7% of white dwarfs possess asteroid belts analogous to the solar system’s. However, two recent surveys of main-sequence solar-type stars find that only 1 star out of 69 (Bryden et al. 2006) or 1 star out of 41 (Beichman et al. 2006) have

warm dust that might be associated with asteroids. While these surveys could not have detected an analog to the current zodiacal cloud in the solar system, our own asteroid belt was probably much more massive in the past, and associated warm dust could have produced a significant infrared excess at $\lambda < 30 \mu\text{m}$ (Gaidos 1999). We show in an Appendix that when the effects of a stellar wind are included, the infrared excess from dust associated with asteroids is suppressed, and therefore, both young and old solar-type main-sequence stars may possess undetected asteroid belts.

2. WHITE DWARF POLLUTION FROM THE INTERSTELLAR MEDIUM?

The accretion of interstellar matter is a plausible source of the external-pollution of some white dwarfs. Here, however, we argue that interstellar accretion cannot explain the measured atmospheric abundances in the three helium-rich white dwarfs listed in Table 1. These stars are taken from the study of Wolff et al. (2002) who report both their own results and summarize previous studies for the hydrogen, carbon, magnesium, silicon, calcium and iron abundances in 10 helium-rich white dwarfs. The element with the smallest error in its abundance determinations is iron (Wolff et al. 2002), and here we focus on abundances relative to this element. For six stars, the carbon abundance is not well enough measured to determine the source of the material. One star, L 119-34, exhibits $n(\text{C})/n(\text{Fe}) \approx 100$, but with very large errors; this star may have experienced dredge-up. The three stars with values of $n(\text{C})/n(\text{Fe})$ more than a factor of 10 below solar are listed in Table 1.

We show in Figure 1 a plot of $\log n(\text{Mg})/n(\text{Fe})$, compared to $\log n(\text{Si})/n(\text{Fe})$, for the Sun (Lodders 2003), CI chondrites (Lodders 2003), L chondrites (Wasson & Kallemeyn 1988), the Earth’s crust (Ronov & Yaroshevsky 1969) and the three white dwarfs listed in Table 1 (Wolff et al. 2002). We only show results for L chondrites; the relative abundances in LL chondrites and H chondrites are within 30% of those in L chondrites (Wasson & Kallemeyn 1988). Together, these three classes of chondrites comprise slightly more than 75% of all meteorite “falls” (Table II-8 in Wasson 1974). Also, we do not display the relative abundances for comet Halley discussed below since they are very close to the meteoritic values (Jessberger et al. 1988).

We see from Figure 1 that relative silicon and magnesium abundances in H 2253+8023 and GD 40 are in agreement with the solar and meteoritic values while the relative abundances for Ross 640 are apparently discrepant. However, given all the uncertainties, the white dwarf abundances shown are consistent with the picture that these stars accrete from the interstellar medium (Wolff et al. 2002). Figure 2 shows a plot of $\log n(\text{Ca})/n(\text{Fe})$ com-

pared to $\log n(\text{Mg})/n(\text{Fe})$. Again, within the large uncertainties, the relative abundances in the atmospheres of the white dwarfs are consistent with accretion of interstellar matter.

We show in Figure 3 a comparison of $\log n(\text{C})/n(\text{Fe})$ with $\log n(\text{Mg})/n(\text{Fe})$ for the same objects as shown in Figures 1 and 2. The LL and H chondrites have values of $\log n(\text{C})/n(\text{Fe})$ similar to that of the L chondrites while all other chondrites have values of $\log n(\text{C})/n(\text{Fe})$ ranging between that of the CI chondrites and that of the L chondrites. Carbon composes only 10^{-4} of the mass of iron meteorites (Lewis & Moore 1971). Figure 3 shows that all three white dwarfs have carbon to iron abundance ratios at least a factor of 10 below solar; a result that is naturally understood if these stars have accreted asteroids with a chondritic composition.

In Figure 3 we also display the results for comet Halley (Jessberger et al. 1988). Its relatively high carbon abundance, which is characteristic of many but not all comets (A’Hearn et al. 1995), means that models for cometary accretion onto these white dwarfs (Alcock et al. 1986) are not supported for Halley analogs. Analogs to Kuiper Belt Objects that are largely composed of ice or other volatiles are not likely to survive the star’s evolution on the Asymptotic Giant Branch (Jura 2004). However, rocky cores of such objects might survive, and ultimately could accrete onto the star after it has evolved into a white dwarf. We do not know if such hypothetical bodies are as carbon-deficient as required by the observed pollutions.

Is it possible to modify the interstellar accretion model to explain the results shown in Figure 3? Because of their low hydrogen abundances, it is usually hypothesized that the externally-polluted helium-rich white dwarfs accrete grains without accreting gas; the hydrogen accretion rate must be suppressed by as much as factor of 10^6 (Friedrich et al. 1999, 2004). Is the interstellar carbon largely in the gas-phase and therefore not accreted? (see Frisch & Slavin 2003, Kimura et al. 2003) The interstellar gas-phase carbon abundance lies between $1.40 \pm 0.20 \times 10^{-4}$ (Cardelli et al. 1996) and $1.61 \pm 0.17 \times 10^{-4}$ (Sofia et al. 2004). The total solar carbon abundance, which may also be the interstellar abundance, is given as $2.45 \pm 0.26 \times 10^{-4}$ by Asplund et al. (2005), but might be as large as 3.3×10^{-4} (Pinsonneault & Delahaye 2006). With these results, it appears that carbon is appreciably distributed in both the gas phase and solid phase. However, the true interstellar abundance may not be solar. The abundance of carbon in early-type stars is inferred to be $1.95 \pm 0.14 \times 10^{-4}$ by Nieva & Przybilla (2006), but, in contrast, Hempel & Holweger (2003) find carbon abundances in such stars often to be greater than solar. In any case, models of interstellar grains require a large amount of carbon in the solid-phase. Zubko et al. (2004) describe 15 possible interstellar grain models in their Table 5, and all require at least 1.90×10^{-4} carbon atoms in the grains. It appears probable that interstellar carbon is very roughly

equally divided between the gas and solid phases, and it is thus unlikely that almost all interstellar carbon is preferentially inhibited from accreting onto white dwarfs.

3. WHITE DWARF POLLUTION BY MINOR BODIES

We now consider the implications of accreting an asteroid and make an order of magnitude estimate of the a pollution event. We therefore neglect three possible complications which could quantitatively change our detailed results but probably do not lead to a qualitative change in our basic scenario for white dwarf accretion. (1) We assume that the outer convection zone is the region where the accreted material is well-mixed. In main-sequence A-type stars, there may be an outer mixing zone which is substantially larger than the outer convection zone (Richer et al. 2000). (2) We use published calculations which assumed spherical symmetry for estimating the diffusion time scale. At least for main-sequence stars, spherical symmetry may be an oversimplification (Vauclair 2004). (3) We implicitly assume a relative simple set of compositional layers in the helium rich white dwarf – an outer envelope and an inner core. Recent astroseismological studies of white dwarfs show that their interiors are more complex than previously assumed (Metcalf 2005). While these new insights have led to a better understanding of the interior structure of white dwarfs, they have not led to a change in the basic paradigm that external pollution explains the presence of metals in the atmospheres of cool white dwarfs.

Consider a pollution event. While a minor body could directly impact a white dwarf, a more likely scenario is that an asteroid strays within the star’s tidal radius. In this case, a flat disk analogous to Saturn’s rings could form (Jura 2003), and the matter then accretes from this ring onto the star. We assume that the externally-donated material from the ring is quickly and uniformly distributed throughout the star’s outer convective envelope which has mass, $M(env)$. We assume that all the polluting elements linger in the atmosphere for the same characteristic settling time, and then the star again appears unpolluted. The convective envelopes of helium-rich white dwarfs are much more massive than those of hydrogen-rich white dwarfs, and therefore the helium-rich white dwarfs require much greater amounts of pollution to produce a detectable abundance anomaly.

We now consider the individual stars in Table 1. For GD 40 and HS 2253+8023 with T_{eff} near 15,000 K we adopt $M(env) = 2 \times 10^{-6} M_{\odot}$ while for Ross 640 with $T_{eff} = 8500$ K we adopt $M(env) = 6 \times 10^{-6} M_{\odot}$ (McDonald et al. 1998). The mass of accreted iron in the outer envelope, $M_{Fe}(env)$, is then derived from the photospheric iron abundances relative to helium, the dominant constituent in the atmosphere, as reported by Wolff et al (2002). The inferred values of $M_{Fe}(env)$ are given in Table 1. If f_{Fe} , the fraction of the accreted

mass that is iron, is ~ 0.2 as found in L chondrites (Wasson & Kallemeyn 1988), then the total inferred parent body mass is $M_{Fe}(env)/f_{Fe}$. The masses of the polluting bodies that produced the current accretion episodes are between $\sim 7 \times 10^{-7} M_{\oplus}$ and $\sim 3 \times 10^{-4} M_{\oplus}$. For comparison, the mass of Ceres, the largest asteroid in the solar system, is $1.6 \times 10^{-4} M_{\oplus}$ (Michalak 2000).

Above we have estimated the mass required to explain a single pollution event; we now estimate the total amount of mass that is required in asteroid belts to explain the available abundance data for externally-polluted helium-rich white dwarfs as a class. We use $f_{accrete}$ to denote the fraction of time that a star exhibits an accretion event and f_{wd} to denote the fraction of white dwarfs with asteroid belts. We cannot independently estimate $f_{accrete}$ and f_{wd} , but only their ratio. In the survey of 800 white dwarfs by Koester et al. (2005) of which $\sim 20\%$ are likely to be helium-rich (Hansen 2004), there are 11 helium-rich white dwarfs with $\log n(\text{Ca})/n(\text{He}) > -8.7$, the calcium abundance in Ross 640. Therefore for the “typical” pollution event, we adopt $(f_{accrete}/f_{wd}) = 0.07$. With $\log n(\text{Ca})/n(\text{He}) = -6.1$, the abundances in HS 2253+8023 are so high that for events with this extreme degree of pollution we adopt $(f_{accrete}/f_{wd}) = 0.01$. We define $M_{accrete}$ as the total mass that a white dwarf accretes during all the pollution episodes that occur during its cooling time. Very approximately:

$$M_{accrete} \approx \frac{M_{Fe}(env)}{f_{Fe}} \frac{t_{cool}}{t_{settl}} \frac{f_{accrete}}{f_{wd}} \quad (1)$$

where t_{cool} denotes the white dwarf’s cooling age taken from Hansen (1999, 2004) and t_{settl} the settling time out of the star’s convective envelope. We adopt $t_{settl} = 5 \times 10^5$ yr (Paquettte et al. 1986, Dupuis et al. 1993a) for all elements at every effective temperature considered here. We list in Table 1 our values of $M_{accrete}$ from equation (1); the results range from $\sim 7 \times 10^{-5} M_{\oplus}$ to $\sim 10^{-3} M_{\oplus}$.

4. DISCUSSION

Before a star becomes a white dwarf, it loses half or more of its main-sequence mass, and the orbits of all the planets and asteroids are altered. Debes & Sigurdsson (2002) have computed that there can be a resulting enhanced rate of asteroids being perturbed into high eccentricity orbits that lead them near enough to the white dwarf for catastrophic disruption to occur. However, it is yet to be demonstrated that enough perturbations of this sort can persist for ~ 1 Gyr as required to explain polluted white dwarfs like Ross 640.

We have suggested that at least 7% of white dwarfs have asteroid belts with total minimum masses of between $\sim 7 \times 10^{-5} M_{\oplus}$ and $\sim 10^{-3} M_{\oplus}$. Since the current mass of the

solar system’s asteroid belt is $\sim 6 \times 10^{-4} M_{\oplus}$ (Krasinsky et al. 2002), the external pollution of white dwarfs can be supplied by asteroid belts analogous to the solar system’s. In the Appendix, we argue that the current evidence that only $\sim 2\%$ of solar-type main-sequence stars exhibit evidence of asteroids does not exclude this proposed scenario.

Carbon abundances are useful for the purpose of distinguishing interstellar from circumstellar accretion. While it is possible to measure values of $n(\text{C})/n(\text{He})$ as low as $\sim 10^{-6}$ for relatively cool helium-rich white dwarfs from the optical C_2 bands (Koester et al. 1982), measurements or upper limits of $n(\text{C})/n(\text{He})$ as low as 10^{-9} around the hotter white dwarfs have required ultraviolet measurements from space-borne telescopes (Wegner & Nelan 1987, Wolff et al. 2002).

The diffusion time of heavy elements out of the atmosphere of a hydrogen-rich white dwarf is typically less than 1000 years. Such polluted stars must be experiencing ongoing accretion. However, the helium-rich stars have much thicker outer convective envelopes, and their diffusion times are correspondingly longer. Polluted helium-rich white dwarfs may not currently exhibit an infrared excess.

A difficulty with the model for accretion of tidally-disrupted asteroids is that some externally-polluted hydrogen-rich white dwarfs do not display any evidence of circumstellar dust (Kilic et al. 2006). It is possible that the dust rings around G29-38 and GD 362 are particularly opaque, analogous to Saturn’s rings, while some white dwarfs have more transparent dust rings or their disks are largely gaseous. In any case, the hypothesis that white dwarfs accrete interstellar grains also leads to the expectation that these stars should display an infrared excess, and therefore the absence of such an excess is not a strong argument in favor of the interstellar accretion model.

5. CONCLUSIONS

The notably low carbon to iron ratios in the atmospheres of three white dwarfs are naturally explained if these stars have accreted carbon-poor asteroids with masses between $7 \times 10^{-7} M_{\oplus}$ and $3 \times 10^{-4} M_{\oplus}$. The inferred existence of extrasolar carbon-deficient minor bodies suggests that chemical and dynamical scenarios for the formation and evolution of rocky planetesimals in the inner solar system can be generalized.

I thank B. Hansen, D. Koester, J. Wasson and B. Zuckerman for valuable conversations. This work has been partly supported by NASA.

REFERENCES

- A'Hearn, M. F., Millis, R. L., Schleicher, D. G., Osip, D. J., & Birch, P. V. 1995, *Icarus*, 118, 223
- Alcock, C., Fristrom, C. C., & Siegelman, R. 1986, *ApJ*, 302, 462
- Ashwell, J. F., Jeffries, R. D., Smalley, B., Deliyannis, C. P., Steinhauer, A., & King, J. R. 2005, *MNRAS*, 363, L81
- Asplund, M., Grevesse, N., Sauval, A. J., Allende Prieto, C., & Bloome, R. 2005, *A&A*, 431, 693
- Becklin, E. E., Farihi, J., Jura, M., Song, I., Weinberger, A. J., & Zuckerman, B. 2005, *ApJ*, 632, L119
- Beichman, C. et al. 2006, *ApJ*, 639, 1169
- Bottke, W. F., Durda, D. D., Nesvorny, D., Jedicke, R., Morbidelli, A., Vokrouhlicky, D., & Levison, H. 2005, *Icarus*, 175, 111
- Bryden, G. et al. 2006, *ApJ*, 636, 1098
- Burns, J. A., Lamy, P. L., & Soter, S. 1979, *Icarus*, 40, 1
- Cardelli, J. A., Meyer, D. M., Jura, M., & Savage, B. D. 1996, *ApJ*, 467,334
- Chayer, P., Vennes, S., Pradhan, A. K., Thejll, P., Beauchamp, A., Fontaine, G., & Wesemael, F. 1995, *ApJ*, 454, 429
- Chen, C. H., Jura, M., Gordon, K. D., & Blaylock, M. 2005, *ApJ*, 623, 493
- Chyba, C. F. 1991, *Icarus*, 92, 217
- Debes, J. H., & Sigurdsson, S. 2002, *ApJ*, 572, 556
- Dominik, C., & Decin, G. 2003, *ApJ*, 598, 626
- Dupuis, J., Fontaine, G., Pelletier, C., & Wasemael, F. 1993, *ApJS*, 84, 73
- Dupuis, J., Fontaine, G., & Wesemael, F. 1993, *ApJS*, 87, 345
- Durda, D. D., & Dermott, S. F. 1997, *Icarus*, 130, 140
- Fixsen, D. J., & Dwek, E. 2002, *ApJ*, 578, 1009

- Friedrich, S., Koester, D., Heber, U., Heffrey, C. S., & Reimers, D. 1999, *A&A*, 350, 865
- Friedrich, S., Jordan, S., & Koester, D. 2004, *A&A*, 424, 665
- Frisch, P., & Slavin, J. 2003, *ApJ*, 594, 844
- Gaidos, E. J. 1999, *ApJ*, 510, 131
- Gail, H.-P. 2002, *A&A*, 390, 253
- Hansen, B. M. S. 1999, *ApJ*, 520, 680
- Hansen, B. M. S. 2004, *Phys. Rept* 399, 1
- Hempel, M. & Holweger, H. 2003, *A&A*, 408, 1065
- Jessberger, E. K., Christoforidis, A., & Kissel, J. 1988, *Nature*, 332, 691
- Jura, M. 2003, *ApJ*, 584, L91
- Jura, M. 2004, *ApJ*, 603, 729
- Kilic, M., von Hippel, T., Leggett, S. K., & Winget, D. E. 2005, *ApJ*, 632, L115
- Kilic, M., von Hippel, T., Leggett, S. K., & Winget, D. W. 2006, *ApJ*, 646, 474
- Kimura, K., Mann, I., & Jessberger, E. K. 2003, *ApJ*, 582, 486
- Koester, D., Rollenhagen, K., Napiwotzki, R., Voss, B., Christlieb, N., Homeier, D., & Reimers, D. 2005, *A&A*, 432, 1025
- Koester, D., Weidemann, V., & Zeidler, E. M. 1982, *A&A*, 116, 147
- Koester, D., & Wilken, D. 2006, *A&A*, 453, 105
- Krasinsky, G. A., Pitjeva, E. V., Vasilyev, M. V., & Yagudina, E. I. 2002, *Icarus*, 158, 98
- Krot, A. N., Fegley, B., Lodders, K., & Palme, H. 2000, in *Protostars and Planets IV*, ed. V. Mannings, A. P. Boss, S. S. Russell (Tucson: University of Arizona Press), 1019
- Laws, C., & Gonzalez, G. 2003, *ApJ*, 595, 1148
- Lewis, C. F., & Moore, C. B. 1971, *Meteoritics*, 6, 195
- Lodders, K. 2003, *ApJ*, 591, 1220
- Lodders, K. 2004, *ApJ*, 611, 587

- MacDonald, J., Hernanz, M., & Jose, J. 1998, MNRAS, 296, 523
- Metcalfe, T. S. 2005, MNRAS, 363, L86
- Michalak, G. 2000, A&A, 360, 363
- Neckel, H. 2000, in Allen's Astrophysical Quantities, ed. A. N. Cox (New York: Springer), 353
- Nieva, M. F., & Przybilla, N. 2006, ApJ, 639, 39
- Nittler, L. R., McCoy, T. J., Clark, P. E., Murphy, M. E., Trombka, J. I., & Jarosewich, E. 2004, Antarctic Meteorite Res. 17, 233.
- Paquette, C., Pelletier, C., Fontaine, G., & Michaud, G. 1986, ApJS, 61, 197
- Pelletier, C., Fontaine, G., Wesemael, F., Michaud, G., & Wegner, G. 1986, ApJ, 307, 242
- Petit, J.-M., Morbidelli, A., & Chambers, J. 2001, Icarus, 153, 338
- Petitclerc, N., Wesemael, F., Kruk, J. W., Chayer, P., & Billeres, M. 2005, ApJ, 624, 317
- Pierce, K. 2000, in Allen's Astrophysical Quantities, ed. A. N. Cox (New York: Springer), 355
- Pinsonneault, M. H., & Delahaye, F. 2006, astro-ph 0606077
- Plavchan, P., Jura, M., & Lipsy, S. J. 2005, ApJ, 631, 1161
- Reach, W. T., Kuchner, M. J., von Hippel, T., Burrows, A., Mullaly, F., Kilic, M., & Winget, D. E. 2005, ApJ, 635, L161
- Richer, J., Michaud, G., & Turcotte, S. 2000, ApJ, 529, 338
- Rieke, G. H. et al. 2005, ApJ, 620, 1010
- Roberge, A., Feldman, P. D., Weinberger, A., Deleuil, M., & Bouret, J.-C. 2006, Nature, 441, 724
- Ronov, A. B., & Yaroshevsky, A. A. 1969, in The Earth's Crust and Upper Mantle, American Geophysical Union, ed. P. J. Hart, 37
- Rybicki, K. R., & Denis, C. 2001, Icarus, 151, 130
- Sackmann, I.-J., & Boothroyd, A. I. 2003, ApJ, 583, 1024

- Simonelli, D. P., Pollack, J. B., & McKay, C. P. 1997, *Icarus*, 125, 261
- Sofia, U. J., Lauroesch, J. T., Meyer, D. M., & Cartledge, S. I. B. 2004, *ApJ*, 605, 272
- Vauclair, S. 2004, *ApJ*, 605, 874
- Wasson, J. T. 1974, *Meteorites* (Berlin: Springer-Verlag)
- Wasson, J. T., & Kallemeyn, G. W. 1988, *Phil. Trans. Roy. Soc. London, A*, 325, 535
- Waters, L. B. F. M., Cote, P., & Geballe, T. R. 1988, *A&A*, 203, 348
- Wegner, G., & Nelan, E. P. 1987, *ApJ*, 319, 916
- Wolff, B., Koester, D., & Liebert, J. 2002, *A&A*, 385, 995
- Wood, B. E., Muller, H.-R., Zank, G.P., Linsky, J. L., & Redfield, S. 2005, *ApJ*, 628, L143
- Zubko, V., Dwek, E., & Arendt, R. G. 2004, *ApJS*, 152, 211
- Zuckerman, B., Koester, D., Reid, I. N., & Hunsch, M. 2003, *ApJ*, 596, 477

APPENDIX

Is there enough mass in asteroid belts around main-sequence stars to account for white dwarf pollutions? Paralleling the discussion by Plavchan et al. (2005) for main-sequence M-type stars, we argue that when the effects of stellar winds are included, infrared excesses from analogs to the Sun’s asteroid belt are difficult to detect even for young main-sequence stars.

Poynting-Robertson drag controls the grain lifetime in the solar system (Burns et al. 1979). However, when a star of luminosity, L_* , has a mass loss rate, \dot{M}_{wind} , sufficiently large such that $\dot{M}_{wind} c^2 > L_*$, as often occurs around stars younger than the Sun, then drag from this wind controls the particle lifetime (Jura 2004, Plavchan et al. 2005). The lifetime, t_{gr} , of a spherical grain of radius b composed of material with density, ρ_{dust} in a circular orbit of radius D exposed to a stellar wind with rate \dot{M}_{wind} in the drag-dominated regime, is (Plavchan et al. 2005):

$$t_{gr} \approx \frac{4 \pi b \rho_{dust} D^2}{3 \dot{M}_{wind}} \quad (\text{A1})$$

With $b = 30 \mu\text{m}$ as representative of particles in the zodiacal cloud of the solar system (Fixsen & Dwek 2002), $D = 3 \text{ AU}$, $\rho_{dust} = 3 \text{ g cm}^{-3}$ and $\dot{M}_{wind} \sim 3 \times 10^{14} \text{ g s}^{-1}$ as characteristic of a vigorous stellar wind (see below), then $t_{gr} \approx 8000 \text{ yr}$. Therefore, the lifetime of dust particles is short compared to the main-sequence age, and the systems quickly relax to a steady state. In this case, the luminosity of the infrared excess, L_{IR} , compared to the stellar luminosity, L_* , is (Jura 2004):

$$L_{IR} \approx \frac{\dot{M}_{dust}}{2 \dot{M}_{wind}} L_* \ln \left(\frac{D_{init}}{D_{final}} \right) \quad (\text{A2})$$

where D_{init} and D_{final} denote the initial and final distances of a dust grain from the host star and \dot{M}_{dust} denotes the dust production rate by asteroidal grinding. Averaging over time and for the moment setting the numerical coefficient equal to unity, we find from (A2) that:

$$\left\langle \frac{L_{IR}}{L_*} \right\rangle \approx \frac{\Delta M_{dust}}{\Delta M_{wind}} \quad (\text{A3})$$

where ΔM_{dust} and ΔM_{wind} denote the total mass in dust produced by asteroids and the total mass lost by a stellar wind. Equation (A3) shows that the fractional infrared excess depends upon the mass in dust created from asteroids compared to the mass lost from the host star.

A promising model for the origin and evolution of the solar system’s asteroids is that the region between Mars and Jupiter initially had $\sim 1 M_{\oplus}$ of planetesimals. After Jupiter formed, this population was dynamically disrupted until perhaps only $0.01 M_{\oplus}$ of material remained after the initial 100 Myr of the solar system (Petit et al. 2001, Bottke et al. 2005). Subsequently, this population of asteroids was slowly reduced by mutual collisions which ultimately lead to dust and produced an infrared excess. If the Sun loses $0.01 M_{\odot}$ in its wind (see below), then we expect a time averaged value of L_{IR}/L_* of $\sim 3 \times 10^{-6}$ which, as illustrated below, is difficult to detect. If the dust production rate is stochastic as has been suggested for the history of the asteroid belt (Durda & Dermott 1997) and for dust production around main-sequence A-type stars (Rieke et al. 2005), then there can be phases when the infrared excess is detectable.

Above, we have discussed some general features of the detectability of asteroids; we now present a specific illustration using conservative estimates for poorly-known quantities. Since dust is produced by collisions, we expect that $\dot{M}_{dust} = C M_{PB}^2$ where M_{PB} is the mass of the asteroid belt and C is a complicated function determined by the composition, size distribution and orbits of the asteroids. Instead of evaluating C from first principles, we adopt an empirical approach and implicitly derive C from the observed rate of dust production in the solar system. This method can explain why we do not frequently detect

analogs to our own asteroid belt; it does not explore the physics of asteroid formation and evolution.

In a simple model C is constant with time (Dominik & Decin 2003) and:

$$\dot{M}_{dust}(t) = \dot{M}_{dust}(t_{Now}) \left(\frac{t_{Now}}{t} \right)^2 \quad (\text{A4})$$

where t_{Now} denotes the current age of the Sun which we take to equal 4.6 Gyr. Alternatively, Gaidos (1999) has suggested that C can be scaled from the history of cratering on the Moon. In this case,

$$\dot{M}_{dust}(t) = \dot{M}_{dust}(t_{Now}) \left(1 + \beta' \exp \left[\frac{t_{Now} - t}{\tau_{cr}} \right] \right) \quad (\text{A5})$$

where $\beta' = 1.6 \times 10^{-10}$ and $\tau_{cr} = 0.144$ Gyr (Chyba 1991). We show a comparison between the two production rates in Figure 4; \dot{M}_{dust} was much larger in the past. We do not show dust production rates for ages less than 100 Myr because these extrapolations are especially uncertain. Equations (A4) and (A5) integrate to yield total dust production from $t = 100$ Myr until now of $\sim 0.003 M_{\oplus}$ and $\sim 0.01 M_{\oplus}$, respectively, for $\dot{M}_{dust}(t_{Now}) = 3 \times 10^6 \text{ g s}^{-1}$ (see below). These integrated dust masses are comparable to the very uncertain estimate of the total amount of mass in asteroids that existed after the first 100 Myr of the solar system.

To assess equation (A2), we need to estimate the spatial motion of the dust. Because the initial and final locations enter only logarithmically, we incorporate very simply the effects of particle collisions and orbiting planets by setting $D_{init} = 3 D_{final}$. To find the specific luminosity, we expect the particles to drift inwards and establish a density variation that scales as D^{-1} and therefore that $L_{IR,\nu}$ ($\text{erg s}^{-1} \text{ Hz}^{-1}$) varies as ν^{-1} over the spectral range where most of the emission is produced (Jura 2004, Waters et al. 1988). In this case:

$$L_{IR,\nu} \approx \frac{\dot{M}_{dust}}{2 \dot{M}_{wind}} \frac{L_{*}}{\nu} \quad (\text{A6})$$

Equation (A6) is valid between a minimum frequency, ν_{min} , and a maximum frequency, ν_{max} given by $\nu_{min} \approx 3 k_B T_{min}/h$ and $3 k_B T_{max}/h$, respectively where the minimum and maximum grain temperatures are determined by D_{init} and D_{final} . Adopting $D_{init} = 3 \text{ AU}$, then a particle that behaves like a black body in orbit around the Sun has a temperature of 160 K implying that the maximum wavelength at which we can use equation (A6) is $\sim 30 \mu\text{m}$.

To estimate the fractional infrared excess, f_{ex} , we compare the emission of the circumstellar dust with the long-wavelength emission from the star's atmosphere, $L_{*,\nu}$, which we

take as:

$$L_{*,\nu} \approx 4 \pi R_*^2 \frac{2 \pi \nu^2 k_B T_* k_{corr}}{c^2} \quad (\text{A7})$$

In equation (A7), we expect that the stellar atmosphere emits on the Rayleigh-Jeans slope but the absolute value of the emission scales from the star’s effective temperature by the factor k_{corr} . For the Sun at 20 μm , we use the central surface brightness (Neckel 2000) and the limb darkening (Pierce 2000) to derive $k_{corr} = 0.84$ which we adopt here.

The mass loss rate from solar-type main-sequence stars are measured for only a handful of stars and are poorly known. Sackmann & Boothroyd (2003) have reviewed the available observations of other stars and also used constraints from helioseismology, the current solar lithium abundance, and the signature of the solar wind irradiation of the lunar surface to infer possible historical mass loss rates from the Sun. They consider 21 models with a total mass loss ranging from 0.01 M_\odot to 0.07 M_\odot . Here, we adopt their most conservative estimate that:

$$\dot{M}_{wind}(t) = \dot{M}_{wind}(0) e\left(-\frac{t}{\tau_{wind}}\right) \quad (\text{A8})$$

where $\dot{M}_{wind}(0) = 8.3 \times 10^{14} \text{ g s}^{-1}$ and $\tau_{wind} = 0.755 \text{ Gyr}$. In this model, the Sun loses 1% of its initial mass. Wood et al. (2005) have recently proposed that the mass loss rates are lower than previously thought among stars of high activity. However, Chen et al. (2005) have found an anti-correlation between the X-ray luminosity and infrared excess at 24 μm of solar-type main sequence stars with ages near $\sim 10 \text{ Myr}$ which might be the result of strong winds associated with X-ray activity also suppressing the infrared emission. Even though it is described as conservative, equation (A8) is highly uncertain.

To estimate the infrared excess, we assume the dust production rate given by equation (A4), and then using (A6) - (A8), we find:

$$f_{ex}(t, \lambda) = \frac{L_{IR,\nu}}{L_{*,\nu}} = \left(\frac{\dot{M}_{dust}(t_{Now})}{\dot{M}_{wind}(0)} \right) \left(\frac{t_{Now}}{t} \right)^2 \left(\frac{\sigma_{SB} T_*^3 \lambda^3}{4 \pi k_{corr} k_B c} \right) e\left(\frac{t}{\tau_{wind}}\right) \quad (\text{A9})$$

where σ_{SB} denotes the Stephan-Boltzmann constant. Making the extreme assumption that all the dust in the zodiacal cloud arises from asteroids, we adopt $\dot{M}_{dust}(t_{Now}) = 3 \times 10^6 \text{ g s}^{-1}$ (Fixsen & Dwek 2002). An equivalent to equation (A9) can be derived for the dust production rate given by equation (A5) instead of equation (A4).

We show in Figure 5 plots of $f_{ex}(24 \mu\text{m})$ to illustrate the infrared excess that might be produced as a function of time. We show results for 24 μm because the dust emission stands out best at the longest wavelengths, as can be seen from equation (A9). Also, the *Spitzer Space Telescope* can observe sensitively at this wavelength. Finally, we are interested in asteroids cooler than 250 K, since any hotter asteroids would probably be destroyed when

the star evolves onto the asymptotic giant branch (see, for example, Rybicki & Denis 2001). Our display in Figure 5 overestimates $f_{ex}(24 \mu\text{m})$ for stars older than 3 Gyr since Poynting-Robertson drag is not included. Also, we do not show $f_{ex}(24 \mu\text{m})$ for stars younger than 100 Myr because the extrapolations are unreliable.

We see in Figure 5 that the infrared excess is unobservable for \dot{M}_{dust} given by equation (A4). However, if the dust production rate follows equation (A5), then when the system is young, the excess may be detectable for a duration of ~ 200 Myr or about 4% of the Sun’s total current age. Thus even if equation (A5) correctly approximates \dot{M}_{dust} , we expect the detection of infrared excesses from asteroids to be rare. The displays in Figure 5 are for a “conservative” estimate of the stellar wind mass loss rate; $f_{ex}(24 \mu\text{m})$ would be lower if the wind is stronger than given by equation (A8).

It is possible that instead of a steady production of dust given by \dot{M}_{dust} there are short, impulsive bursts from destruction of large asteroids. We now present a schematic description of how this might affect the observability of infrared excesses. We denote the instantaneous dust formation rate by \dot{M}_{inst} . We assume that for times long compared to the particle decay time given by equation (A1) but short compared to the stellar evolution time that $\langle \dot{M}_{inst} \rangle$ equals \dot{M}_{dust} . We also assume that during a stochastic event when the particle decay time is relatively short compared to the time that it takes for an asteroid to be fully pulverized, the infrared excess can be derived from the instantaneous dust decay rate and equation (A2).

Let $f_{det}(\lambda)$ denote the threshold for detecting an excess at wavelength λ . If $p(t, \lambda)$ denotes the probability that an excess is detectable at epoch t , then we adopt $p(t, \lambda) = 1$ if $f_{ex} > f_{det}$. If, however, \dot{M}_{dust} is too small for an excess to be detected during steady dust production, a stochastic mass loss event can be detected if \dot{M}_{inst} is sufficiently large during a relatively short time. Using the dependence of the excess infrared luminosity on the dust production rate given by equation (A2), and averaging over a time long compared to the individual particle decay time but short compared to the stellar evolutionary time, then when $f_{ex} < f_{det}$, we write that:

$$p(t, \lambda) \leq \frac{f_{ex}(t, \lambda)}{f_{det}(\lambda)} \tag{A10}$$

Assuming that $f_{det}(\lambda) = 0.02$ independent of wavelength and denoting p_{max} as the maximum possible value of p , we show in Figure 6 a plot of $\langle p_{max}(\lambda) \rangle$ between 0.1 Gyr and 4.6 Gyr for mean dust production rates given by equations (A4) and (A5).

If equation (A4) exactly describes the dust production rate, then, as seen in Figure 5, the excess is never detectable. If, however, the dust is released in short bursts and equation (A4) only describes the mean loss rate, then as can be seen in Figure 6, there is a small

probability that an excess can be detected. We can also see from Figure 6 that if equation (A5) describes the dust production rate then during as much as 10% of the time between 0.1 and 4.6 Gyr, a Sun-like star exhibits an infrared excess at $24 \mu\text{m}$ produced by asteroid destruction.

Although there are many poorly known quantities, Figures 5 and 6 illustrate the basic result contained within equation (A3). As long as the time-averaged mass in dust produced by asteroids is small compared to the time-averaged mass lost from the star as we infer for our solar system, the expected infrared excess is usually undetectable.

Table 1 – Helium-Rich White Dwarfs With Low $n(\text{C})/n(\text{Fe})$

Star	t_{cool} (Gyr)	$M_{Fe}(env)$ (10^{22} g)	$M_{accrete}$ (10^{24} g)
Ross 640	0.7	0.08	0.4
GD 40	0.2	4	6
HS 2253+8023	0.2	40	8

Here, $M_{Fe}(env)$ denotes the mass of iron currently in the convective envelope while $M_{accrete}$ is taken from equation (1).

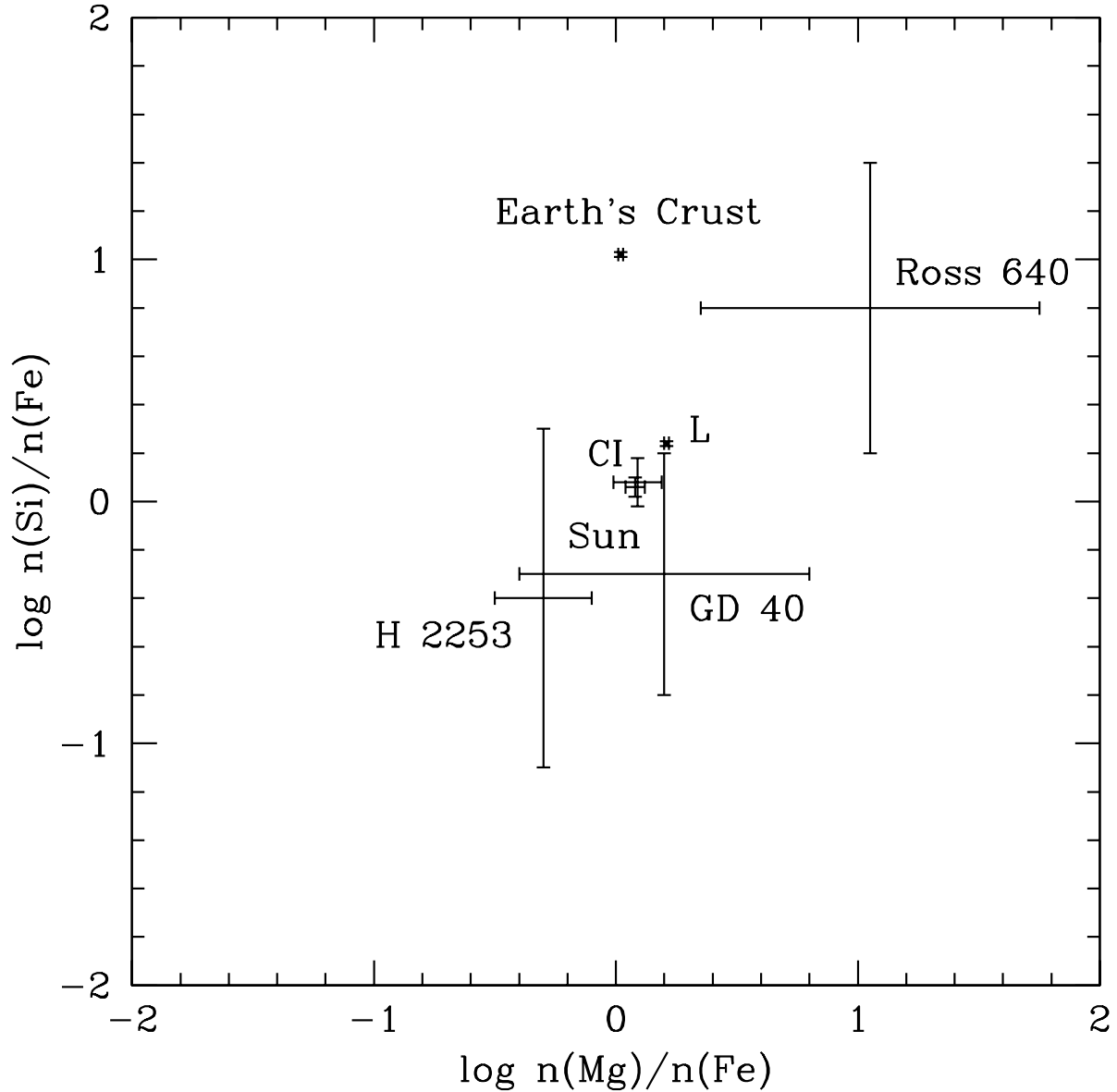


Fig. 1.— Values of $\log n(\text{Mg})/n(\text{Fe})$ and $\log n(\text{Si})/n(\text{Fe})$ for the Sun, CI chondrites (labeled CI), L chondrites (labeled L) the Earth's crust, and three white dwarfs. We do not display errors bars for the measured abundances in the L chondrites or the Earth's crust because they are not supplied by the authors of these studies; Nittler et al. (2004) report $\sim 20\%$ abundance variations among different L chondrites.

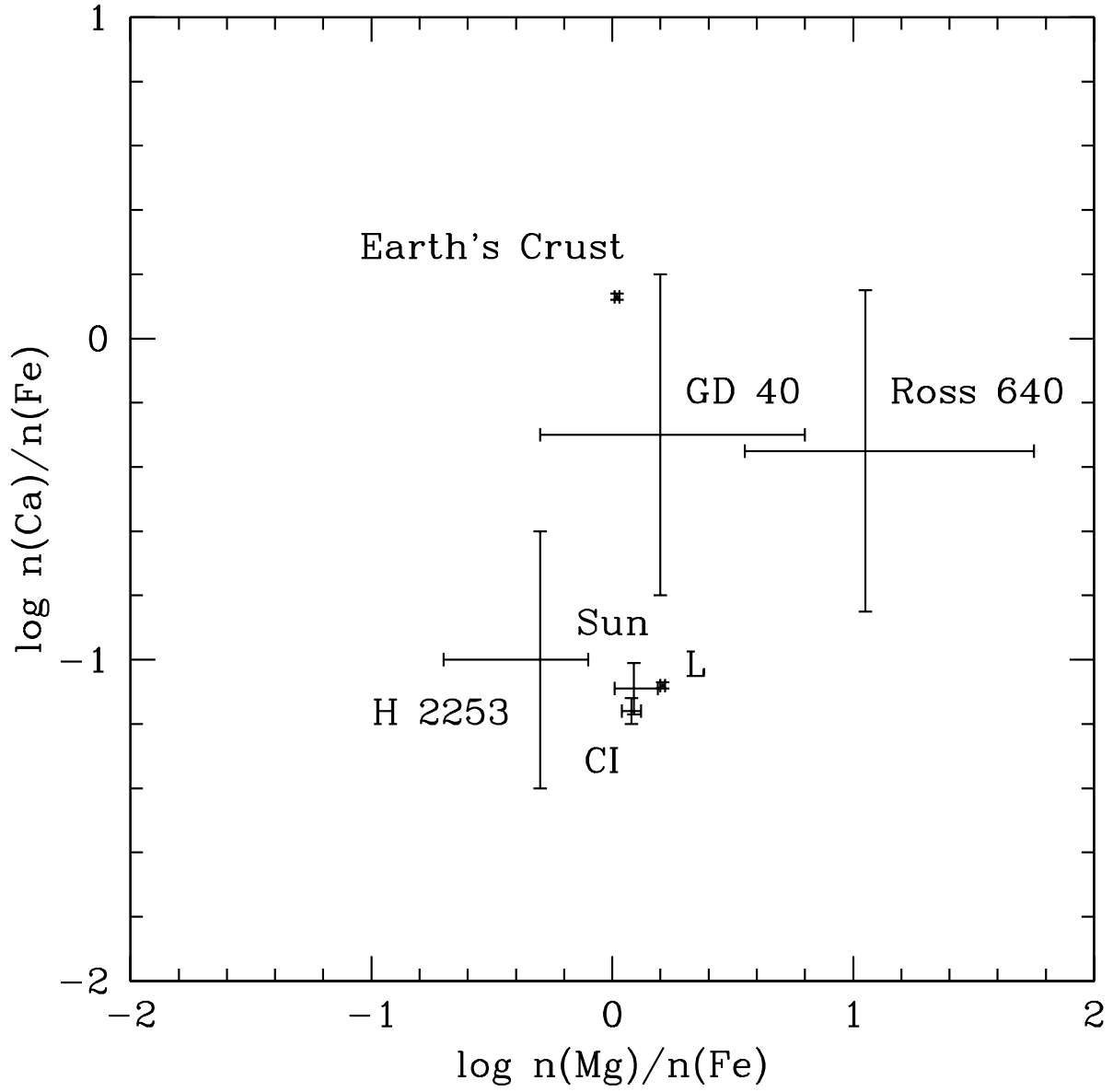


Fig. 2.— Similar to Figure 1 except that values of $\log n(\text{Ca})/n(\text{Fe})$ are compared with those of $\log n(\text{Mg})/n(\text{Fe})$.

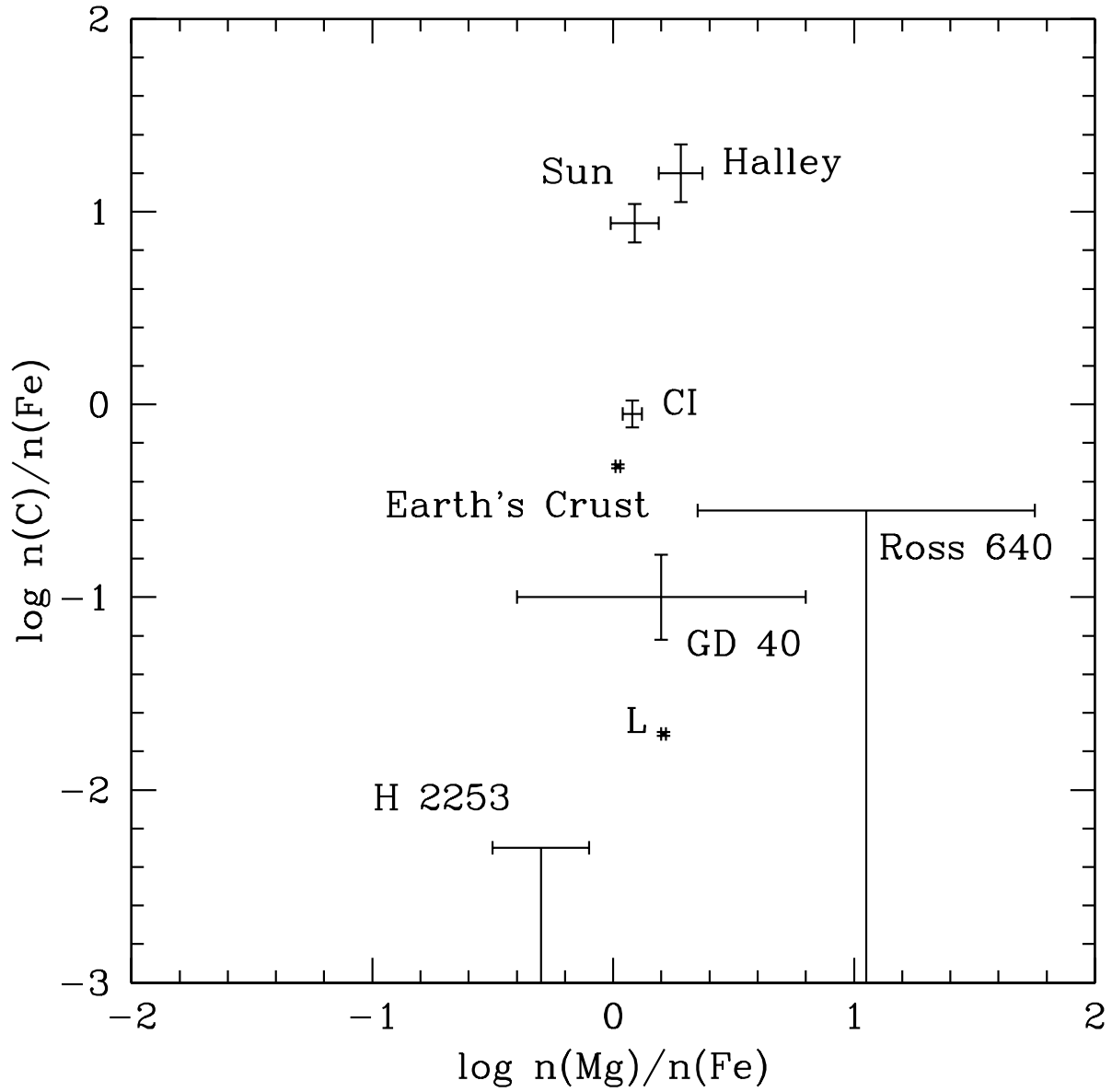


Fig. 3.— Similar to Figure 1 except that values for $\log n(C)/n(Fe)$ are compared with those of $\log n(Mg)/n(Fe)$. We have added a point for the average composition of comet Halley determined by the mass spectrometer on the VEGA-1 spacecraft (Jessberger et al. 1988).

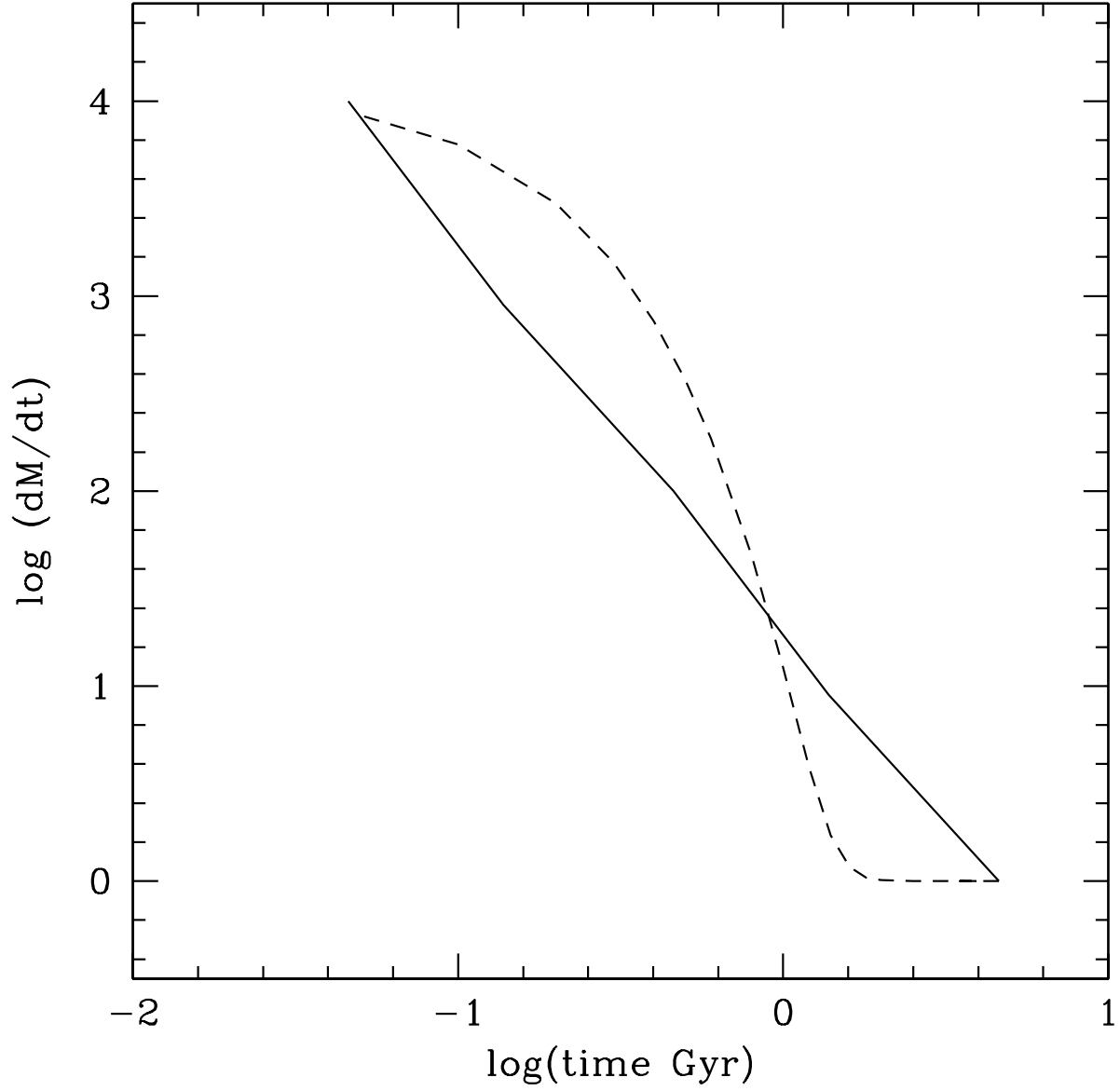


Fig. 4.— Dust production rate as a function of time normalized to the current epoch. The solid and dashed lines are derived from equations (A4) and (A5), respectively.

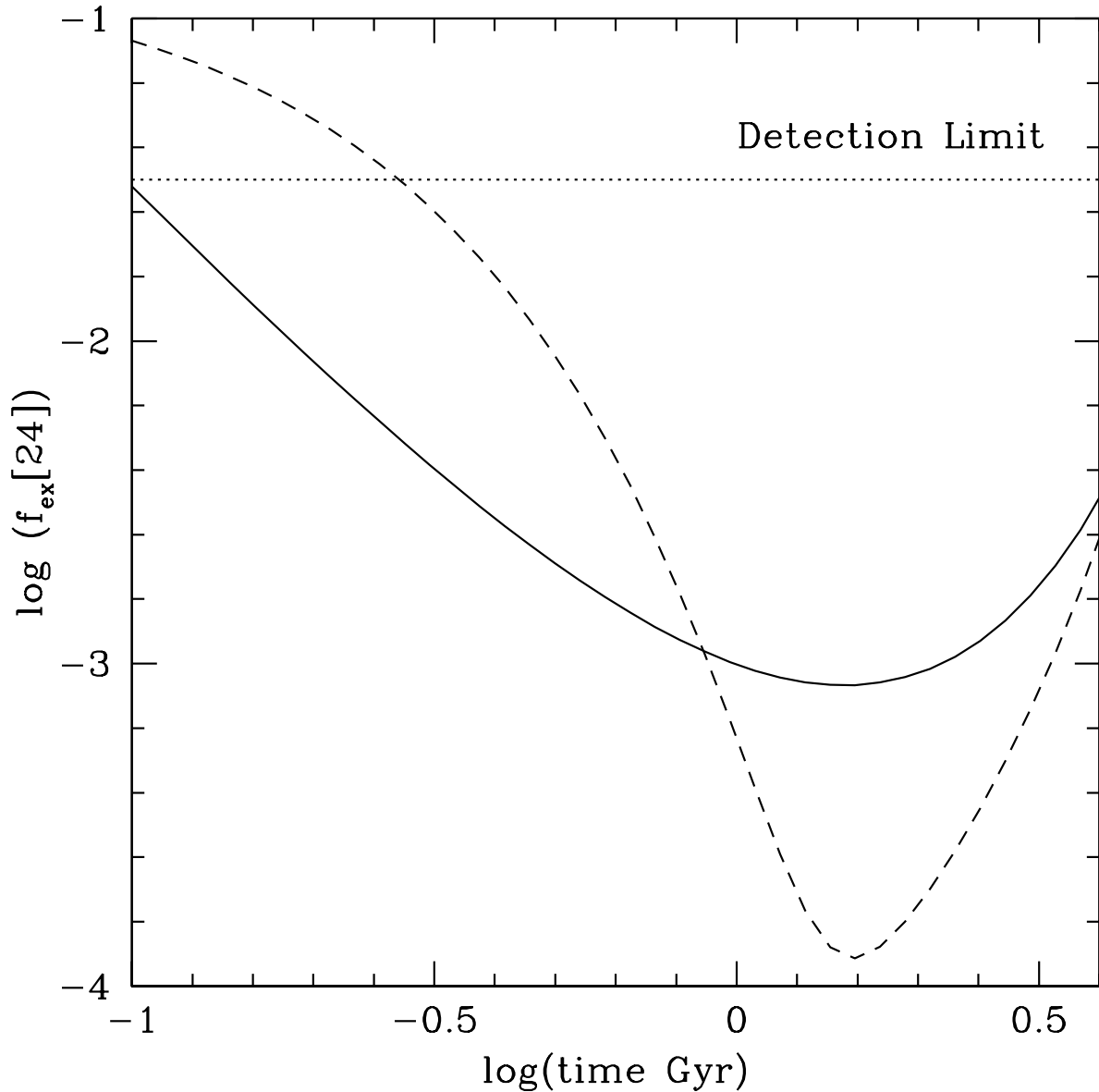


Fig. 5.— Fractional excess at $24 \mu\text{m}$ as a function of time from equation (A9) for a Sun-like star ($L = 1 L_{\odot}$ and $T_{*} = 5780 \text{ K}$) with the mass loss and dust production parameters given in the text shown by the solid line. The dashed line is the same except that we assume the dust production rate is given by equation (A5) instead of equation (A4). Infrared excesses may be detectable for $\log f_{\text{exc}}[24] > -1.5$ (Beichman et al. 2006, Bryden et al. 2006, Rieke et al. 2005)

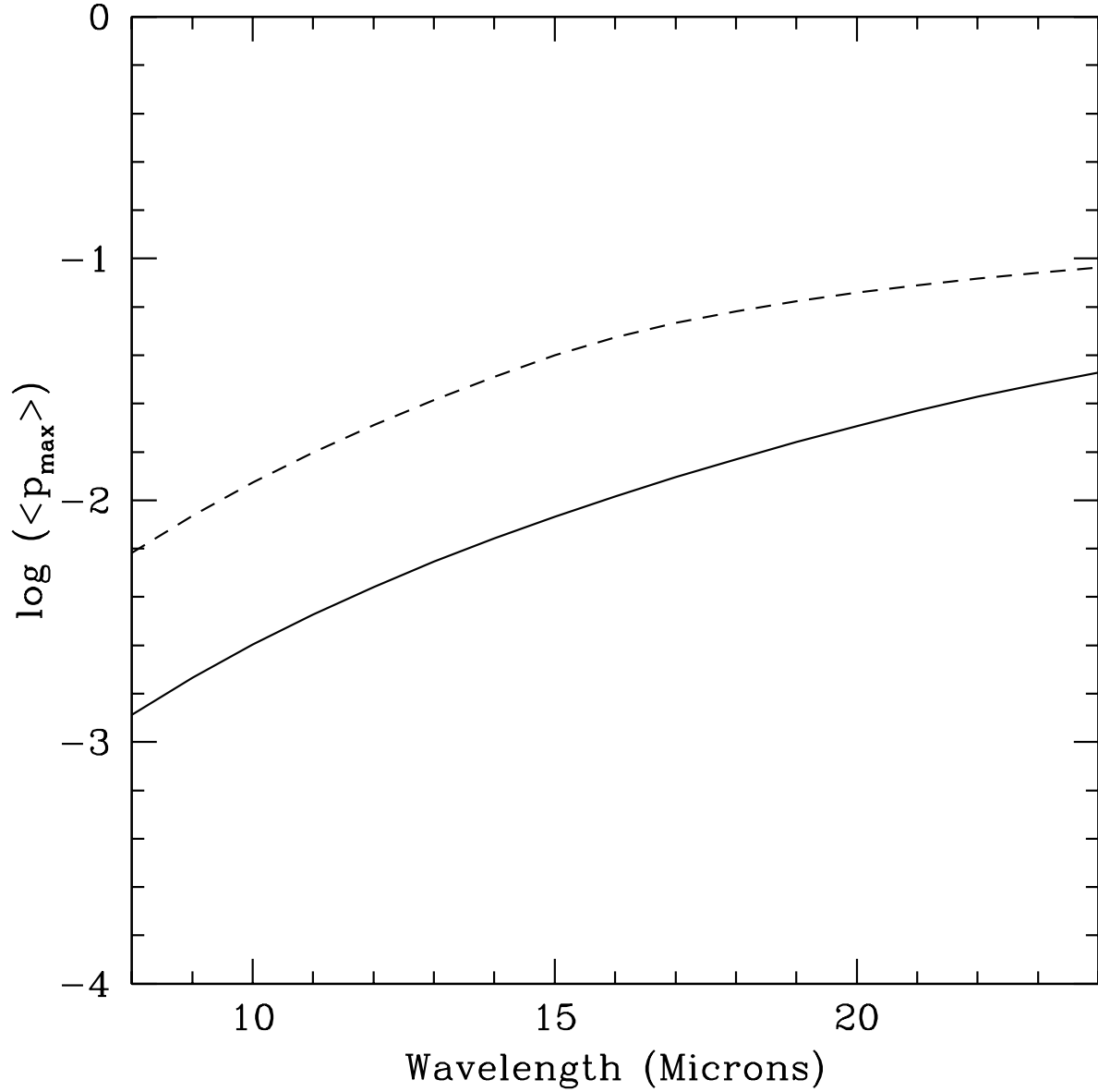


Fig. 6.— Logarithm of the maximum probability of detecting an infrared excess as a function of observing wavelength during the time interval 0.1 Gyr to 4.6 Gyr from equation (A10). The solid and dashed lines are for mean asteroidal dust production rates from equations (A4) and (A5), respectively.